

# The enormous abundance of D<sub>2</sub>CO in IRAS 16293–2422

L. Loinard<sup>1</sup>, A. Castets<sup>2</sup>, C. Ceccarelli<sup>3</sup>, A.G.G.M. Tielens<sup>4</sup>, A. Faure<sup>3</sup>, E. Caux<sup>5</sup>, and G. Duvert<sup>3</sup>

<sup>1</sup> Institut de Radio Astronomie Millimétrique, 300 rue de la piscine, 38406 St. Martin d'Hères, France

<sup>2</sup> Observatoire de l'Université de Bordeaux I, B.P. 89, 33270 Floirac, France

<sup>3</sup> Laboratoire d'Astrophysique, Observatoire de Grenoble, B.P. 53, 38041 Grenoble Cedex 09, France

<sup>4</sup> SRON, P.O. Box 800, 9700 AV Groningen, The Netherlands

<sup>5</sup> CESR, CNRS-UPS, B.P. 4346, 31028 Toulouse Cedex 04, France

Received 7 April 2000 / Accepted 16 May 2000

**Abstract.** Ceccarelli et al. (1998) recently reported the detection of D<sub>2</sub>CO in the low-luminosity protostar IRAS 16293–2422. Using the data available at the time, they found that the abundance of D<sub>2</sub>CO might be as high as 1/10th that of its hydrogenated counterpart H<sub>2</sub>CO. Here we describe and analyse new multi-transition observations of D<sub>2</sub>CO, HDCO, H<sub>2</sub>CO, and H<sub>2</sub><sup>13</sup>CO towards IRAS 16293–2422. Correcting for the opacity of the H<sub>2</sub>CO lines, we find that the abundance of D<sub>2</sub>CO is  $\sim$  5% that of H<sub>2</sub>CO. In addition, we find a component in absorption – also associated to IRAS 16293–2422, but at larger radius – where the abundance of D<sub>2</sub>CO compared to H<sub>2</sub>CO could be even higher.

Though slightly lower than initially claimed, the abundance of D<sub>2</sub>CO in IRAS 16293–2422 is extremely high, more than one order of magnitude higher than in Orion KL, the only other source where D<sub>2</sub>CO has ever been detected. Because the gas temperature ( $T = 20$ – $50$  K) is too high, deuteration in the gas-phase is very insufficient to explain such high abundances. We conclude that D<sub>2</sub>CO is most likely *not* currently formed in the gas phase, but is evaporated from the dust grains, where it has been accumulating during the cold, dense pre-collapse period.

**Key words:** stars: formation – ISM: abundances – ISM: molecules – ISM: individual objects: IRAS 16293-2422

## 1. Introduction

While singly deuterated molecular species can be fairly easily formed in detectable amounts in the interstellar medium, the formation of multiply deuterated molecules requires more unusual chemistry (Tielens 1983, Brown & Millar 1989, Willacy & Millar 1998). Until recently, the doubly deuterated form of formaldehyde (D<sub>2</sub>CO) was the only multiply deuterated molecule ever detected in space; but recently, the doubly deuterated ammonia (NHD<sub>2</sub>) was also discovered (Roueff et al. 2000). The chemistry leading to the formation of those two species remains poorly understood, but might prove very important to our understanding of interstellar chemistry in general. D<sub>2</sub>CO

was first discovered in Orion KL by Turner (1990), where its relative abundance<sup>1</sup> was found to be  $\sim$  0.3%. Subsequently, it was detected in the low-luminosity protostar IRAS 16293–2422 (Ceccarelli et al. 1998) with a relative abundance possibly as high as 10%. This value however, was derived from only a few lines of D<sub>2</sub>CO and did not account for the opacity of the H<sub>2</sub>CO lines. Here, we use new, multi-transition observations of D<sub>2</sub>CO, HDCO, H<sub>2</sub>CO, and H<sub>2</sub><sup>13</sup>CO obtained towards IRAS 16293–2422 to derive much more accurate values of the relative abundances of D<sub>2</sub>CO, HDCO, and H<sub>2</sub>CO.

## 2. Observations

We conducted a spectral survey towards IRAS 16293–2422, targeting several transitions of D<sub>2</sub>CO, HDCO, H<sub>2</sub>CO, and H<sub>2</sub><sup>13</sup>CO. The transitions were chosen to cover the widest possible range of upper level energies (from  $E_u = 10$  to 100 K). Their wavelengths were between 0.8mm and 2mm, so two telescopes had to be used. The lines lying in the 1mm and 2mm bands were observed with the IRAM 30m telescope, and the higher frequency (0.8mm) transitions with the JCMT 15m telescope (see Table 1). All the observations were made in position switching mode, with the reference position located at  $\Delta\alpha = -180''$ ,  $\Delta\delta = 0''$  from the nominal center of IRAS 16293–2422 at  $\alpha(2000.0) = 16^{\text{h}}24^{\text{m}}22^{\text{s}}.6$ ,  $\delta(2000.0) = -24^{\circ}28'33''.0$ . The intensities reported here are expressed in units of *main beam brightness temperature*. The integration times were chosen to provide adequate signal-to-noise ratios for each line, and ranged from a few minutes for the strongest H<sub>2</sub>CO lines to about 1 hour for the faintest D<sub>2</sub>CO lines. The absolute accuracy of the observations is better than 10% for the data in the 1 and 2mm bands and better than 15% for the data at 0.8mm. The pointing was checked regularly, and found to be accurate to better than 5'' and 3'' for the IRAM and JCMT observations respectively.

*IRAM Observations.* The IRAM observations were performed from 1999 January 8 to 12 with the 30-meter single-dish tele-

<sup>1</sup> Here, and in all the paper, the term *relative abundance* is used to denote the abundance ratio between a deuterated species and its hydrogenated counterpart.

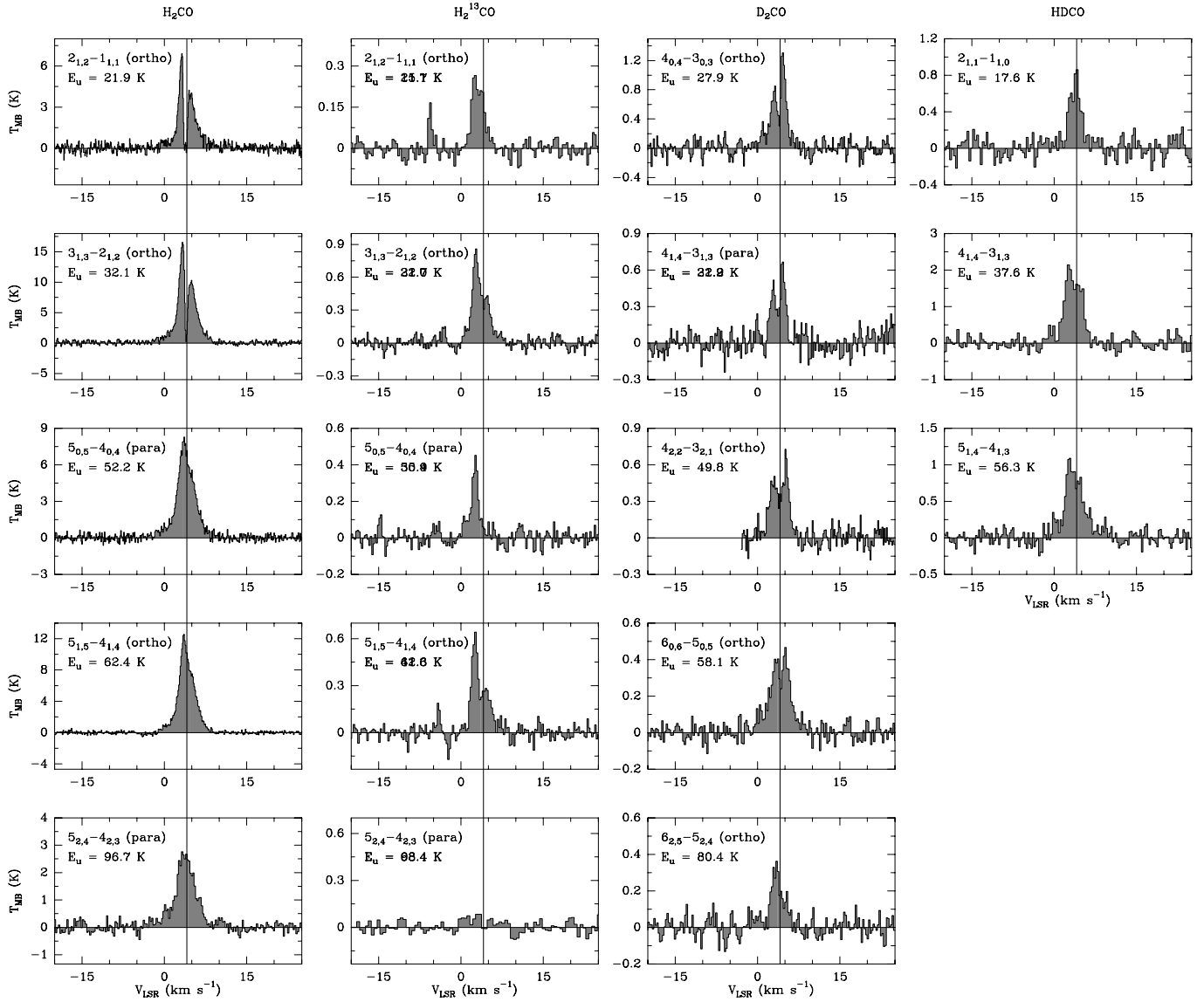


**Fig. 1.** Spectra of all the lines observed towards IRAS 16293–2422. First column: H<sub>2</sub>CO; second column; H<sub>2</sub><sup>13</sup>CO; third column: D<sub>2</sub>CO; and fourth column: HDCO. The spectra are ordered by increasing upper level energies, from top to bottom. The vertical lines indicate the systemic velocity of the source at  $V_{LSR} = 4.2 \text{ km s}^{-1}$ . While odd  $K_{-}$  lines correspond to ortho transitions for the non-deuterated forms of formaldehyde, they correspond to para transitions for D<sub>2</sub>CO because the nucleus of deuterium is a boson, while that of hydrogen is a fermion; HDCO obviously does not have ortho or para transitions.

scope located at an altitude of 2,920 meters on Pico Veleta near Granada in Southern Spain. The 1.3mm and the 2mm SIS receivers available at the time on the 30-meter were used to observe simultaneously at least two spectral lines. The image sideband rejection was always higher than 10 dB; typical system temperatures throughout the run were 200–400 K. The main beam efficiency  $\eta_{mb}$  of the 30-meter is about 0.5 at 1mm, and 0.6 at 2mm; its beamsize is about 10–12'' at 1mm, and 15–17'' at 2mm. The receivers were connected to autocorrelator units providing 80 MHz of bandwidth for a spectral resolution of 80 kHz, this yields velocity resolutions of about 0.1 and 0.08  $\text{km s}^{-1}$  at 1mm and 2mm respectively.

*JCMT Observations.* The JCMT<sup>2</sup> observations targetted the transitions in the 0.8mm band, and were performed from 1999 July 19 to 24. The JCMT is a 15-meter single dish telescope located at an altitude of 4,100 meters near the summit of Mauna Kea in Hawaii. The observations were made with the single-sideband dual-polarization B3 receiver. Typical system temperatures throughout the run were 400–800 K; the main-beam efficiency of the JCMT in the 0.8mm band is about 0.62, and the beamwidth 14–15''. Each polarization of the receiver was con-

<sup>2</sup> The JCMT is operated by the Royal Observatories on behalf of the Particle Physics and Astronomy Research Council of the United Kingdom, the Netherlands Organization for Scientific Research, and the National Council of Canada.

**Table 1.** List of the lines of formaldehyde observed towards IRAS 16293–2422, together with the relevant parameters.

Molecule	Transition	$E_u$ (K)	$\nu$ (GHz)	Instrument	$\Delta\theta$ ( $''$ )	$\eta_{mb}$	$\Delta v$ ( $\text{km s}^{-1}$ )	$\int T_{MB} dv$ ( $\text{K km s}^{-1}$ )
D <sub>2</sub> CO	4 <sub>0,4</sub> –3 <sub>0,3</sub>	27.9	231.410	IRAM-30m	11	0.46	0.10	3.0
	4 <sub>1,4</sub> –3 <sub>1,3</sub>	31.9	221.191	IRAM-30m	11	0.48	0.10	1.6
	4 <sub>2,2</sub> –3 <sub>2,1</sub>	49.8	236.102	IRAM-30m	11	0.68	0.10	1.9
	6 <sub>0,6</sub> –5 <sub>0,5</sub>	58.1	342.522	JCMT-15m	14	0.62	0.13	1.9
	6 <sub>2,5</sub> –5 <sub>2,4</sub>	80.4	349.631	JCMT-15m	14	0.62	0.13	1.0
HDCO	2 <sub>1,1</sub> –1 <sub>1,0</sub>	17.6	134.284	IRAM-30m	17	0.65	0.08	1.8
	4 <sub>1,4</sub> –3 <sub>1,3</sub>	37.6	246.925	IRAM-30m	11	0.68	0.08	7.6
	5 <sub>1,4</sub> –4 <sub>1,3</sub>	56.3	335.097	JCMT-15m	14	0.62	0.14	4.5
H <sub>2</sub> CO	2 <sub>1,2</sub> –1 <sub>1,1</sub>	21.9	140.839	IRAM-30m	17	0.65	0.08	16.6
	3 <sub>1,3</sub> –2 <sub>1,2</sub>	32.1	211.211	IRAM-30m	11	0.45	0.11	43.8
	5 <sub>0,5</sub> –4 <sub>0,4</sub>	52.2	362.736	JCMT-15m	14	0.62	0.13	28.9
	5 <sub>1,5</sub> –4 <sub>1,4</sub>	62.4	351.768	JCMT-15m	14	0.62	0.13	38.3
	5 <sub>2,4</sub> –4 <sub>2,3</sub>	96.7	363.946	JCMT-15m	15	0.62	0.13	11.9
H <sub>2</sub> <sup>13</sup> CO	2 <sub>1,2</sub> –1 <sub>1,1</sub>	21.8	137.450	IRAM-30m	17	0.65	0.08	0.58
	3 <sub>1,3</sub> –2 <sub>1,2</sub>	31.7	206.132	IRAM-30m	11	0.45	0.11	1.60
	5 <sub>0,5</sub> –4 <sub>0,4</sub>	51.0	353.812	JCMT-15m	14	0.62	0.13	0.60
	5 <sub>1,5</sub> –4 <sub>1,4</sub>	61.4	343.325	JCMT-15m	14	0.62	0.14	1.37
	5 <sub>2,4</sub> –4 <sub>2,3</sub>	98.6	354.899	JCMT-15m	15	0.62	0.13	$\lesssim 0.30$

nected to a unit of the DAS autocorrelator providing a bandwidth of 250 MHz for a spectral resolution of 156 kHz. At 0.8mm, this yields a velocity resolution of about 0.13–0.14  $\text{km s}^{-1}$ . The response of the receiver to the two polarizations was checked to be consistent within better than 10%.

### 3. Results and analysis

#### 3.1. Abundance ratios

To derive the physical parameters (temperature and column density) from the observations, we use rotational diagrams. We briefly remind below the basics of this method and refer the reader to Goldsmith & Langer (1999) for a more complete description.

For an optically thin line, the column density in the upper level ( $N_u$ ) can be written as:

$$N_u = \frac{8\pi k\nu^2}{hc^3 A_{u,l}} \times W \quad (1)$$

where  $k$ ,  $h$  and  $c$  have their usual meanings, and where  $\nu$ ,  $A_{u,l}$ , and  $W$  are respectively the frequency, the Einstein coefficient, and the integrated intensity of the line. Under Local Thermodynamic Equilibrium (LTE) conditions, the levels are populated following a Boltzmann law at the gas temperature  $T$ . The resulting relative populations of the energy levels are given by:

$$N_u = \frac{N}{Z} g_u e^{-E_u/kT} \quad (2)$$

where  $N$  is the total column density,  $Z$  the partition function, and  $g_u$  and  $E_u$  are the statistical weight and the energy of the upper

level respectively. Taking the logarithm of Eq. (2), we obtain the basic equation of the rotational diagram method:

$$\ln \frac{N_u}{g_u} = \ln N - \ln Z - \frac{E_u}{kT} \quad (3)$$

Indeed, if one plots the logarithm of the column density in each level (deduced from the observations using Eq. (1)) normalized by the statistical weight, as a function of the energy of the upper level (in effect, building the rotational diagram), one should get a straight line, where the inverse of the slope gives the rotational temperature (which, under LTE conditions, is equal to the kinetic temperature), and where the intersect with the ordinate axis gives the total column density.

To use this method, however, the lines have to be optically thin. To measure the opacity of the H<sub>2</sub>CO lines, we observed both H<sub>2</sub>CO and its less abundant isotopomer H<sub>2</sub><sup>13</sup>CO (Table 1; Fig. 1). The H<sub>2</sub>CO/H<sub>2</sub><sup>13</sup>CO line intensity ratios are of the order of 20–25 for the ortho transitions, and of the order of 40–50 for the para transitions. Though the low-energy transitions show strong absorption features, those values imply only moderate optical depth ( $\tau = 0.3$ –0.7).

The rotational diagram for H<sub>2</sub>CO (Fig. 2) was built after correcting the H<sub>2</sub>CO line intensities for optical depth effects assuming an intrinsic <sup>12</sup>C/<sup>13</sup>C ratio of 60 (Langer et al. 1984, Keene et al. 1998), and an ortho to para ratio of 3. It yields a temperature of 45 K, and a column density  $N(\text{H}_2\text{CO}) = 3.8 \times 10^{14} \text{ cm}^{-2}$ . These values are somewhat different from those reported by van Dishoeck et al. (1995– hereafter VBJG95):  $T = 80 \text{ K}$ ,  $N = 2.1 \times 10^{14} \text{ cm}^{-2}$  using different H<sub>2</sub>CO observations. The difference in temperature is due to the use by VBJG95 of observations covering a wider range of upper level energies (up to 250 K instead of 100 K here). Ignoring the data corresponding to transitions with upper level energies higher than 150 K, the

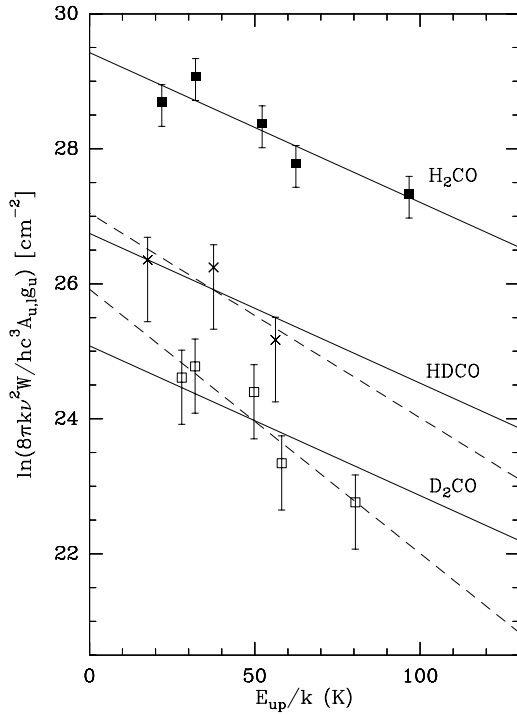


**Fig. 2.** Population diagrams for H<sub>2</sub>CO (filled squared, top) corrected for opacity, HDCO (crosses, middle), and D<sub>2</sub>CO (open square, bottom). The solid lines correspond to the best fits to the data, where the temperature is fixed to the value deduced from the H<sub>2</sub>CO data ( $T = 45$  K), while the dashed lines correspond to fits where the temperature is left as a free parameter.

data of VBJG95 imply a temperature of about 50 K, similar to that found here. As shown by Ceccarelli et al. (2000), while the low-lying transitions originate in an extended, relatively cool component, the higher energy transitions emanate only from the very central regions where the temperature is higher. Since all our HDCO and D<sub>2</sub>CO data cover the upper-level energy range 10–100 K, the abundance ratios are more meaningful if only a similar range of upper-level energy is considered when the column density is derived from the H<sub>2</sub>CO data. Finally, the difference in the column density between VBJG95 and us is a combination of differing angular resolutions and the account for opacity effects not included in VBJG95.

Given the low opacity of the H<sub>2</sub>CO lines, the optical depth of the less abundant species HDCO and D<sub>2</sub>CO are mostly negligible, and no correction is needed<sup>3</sup>. A fit to the data with a temperature  $T = 45$  K deduced from the H<sub>2</sub>CO (solid lines on Fig. 2) yields  $N(\text{HDCO}) = 5.2 \times 10^{13} \text{ cm}^{-2}$  and  $N(\text{D}_2\text{CO}) = 1.9 \times 10^{13} \text{ cm}^{-2}$ . Interestingly, however, when the temperature is left as a free parameter, the HDCO data yield  $T = 33$  K, and the D<sub>2</sub>CO data  $T = 26$  K (dashed lines on Fig. 2). The column densities deduced from the fits with the temperature left as a free parameter are, however, essentially similar to those with the temperature fixed to 45 K because the modification of

<sup>3</sup> We searched for a D<sub>2</sub><sup>13</sup>CO line, and could not detect it, setting an upper limit of  $10^{-2}$  on the opacity of the D<sub>2</sub>CO.

the value of the intercept with the ordinate axis is compensated by the modification of the value of the partition function. They are:  $N(\text{HDCO}) = 4.8 \times 10^{13} \text{ cm}^{-2}$  and  $N(\text{D}_2\text{CO}) = 1.9 \times 10^{13} \text{ cm}^{-2}$ . The improvements in the r.m.s. between the data points and the fits are of 30% and 160% for the HDCO and D<sub>2</sub>CO respectively. Finally, fits with a temperature fixed at 80 K (as found by VBJG95) yield poorer agreement with the data, and column densities of  $N(\text{H}_2\text{CO}) = 5.0 \times 10^{14} \text{ cm}^{-2}$ ,  $N(\text{HDCO}) = 8.1 \times 10^{13} \text{ cm}^{-2}$ , and  $N(\text{D}_2\text{CO}) = 2.7 \times 10^{13} \text{ cm}^{-2}$ . All the fits yield very similar values of the relative abundances between the three isotopomers of formaldehyde (Table 2):

$[\text{HDCO}]/[\text{H}_2\text{CO}]$	$\sim$	13–16%
$[\text{D}_2\text{CO}]/[\text{H}_2\text{CO}]$	$\sim$	5–6%
$[\text{D}_2\text{CO}]/[\text{HDCO}]$	$\sim$	33–40%

### 3.2. Line profiles

The low-lying H<sub>2</sub>CO lines show deep absorptions at the systemic velocity of the source. However, the ratios between their intensities and that of the corresponding H<sub>2</sub><sup>13</sup>CO lines imply only moderate optical depth. The most likely explanation is thus that the absorption originates in cold foreground material. Further support for this idea comes, first, from the fact that the relative absorption is much stronger for the low-lying transitions than for the higher energy lines, indicating that the absorbing material is at a quite lower temperature than the background source; and, second, from the fact that the H<sub>2</sub><sup>13</sup>CO lines show similarly double-peaked profiles. The only exception is the ortho 5<sub>0,5</sub>–4<sub>0,4</sub> line of H<sub>2</sub><sup>13</sup>CO where the red peak is absent – we do not have any explanation for this at the moment.

The D<sub>2</sub>CO lines are also double-peaked. Interestingly, however, the relative depth of the dip at the systemic velocity is nearly constant with the energy of the transition. For H<sub>2</sub>CO, the 2<sub>1,2</sub>–1<sub>1,1</sub> transition ( $E_u = 22$  K) falls to zero, while for the 5<sub>1,5</sub>–4<sub>1,4</sub> transition ( $E_u = 62$  K), it is barely visible. For D<sub>2</sub>CO, on the other hand, the dip of the 4<sub>0,4</sub>–3<sub>0,3</sub> line ( $E_u = 28$  K) and that of the 6<sub>0,6</sub>–5<sub>0,5</sub> transition ( $E_u = 58$  K) are almost of the same intensity. It is likely that the absorption is also due to cold foreground material – possibly the same material responsible for the H<sub>2</sub>CO absorption.

To study this absorption feature, we measured the intensity of the H<sub>2</sub>CO and D<sub>2</sub>CO dips by fitting a gaussian to the profiles *outside* of the absorption, and making the difference between that gaussian fit and the observed spectrum. The derived intensities were used to build the rotational diagrams corresponding to the absorbing gas. Its temperature is found to be about 20 K, in good agreement with the qualitative discussion above: the absorption feature corresponds to a gas at a temperature somewhat smaller than that found for the H<sub>2</sub>CO, but close to that deduced from the D<sub>2</sub>CO. The column densities for the component in absorption are  $N(\text{H}_2\text{CO}) = 4 \times 10^{13} \text{ cm}^{-2}$  and  $N(\text{D}_2\text{CO}) = 5 \times 10^{12} \text{ cm}^{-2}$ . This corresponds to an abundance ratio of about 12%, more than twice that on source.

The distance between the absorbing gas and the source can obviously not be estimated from our observation. However,

**Table 2.** Results of the rotational diagram fits.

	Temperature	Column densities ( $10^{14} \text{ cm}^{-2}$ )			Abundance ratios	
		H <sub>2</sub> CO	HDCO	D <sub>2</sub> CO	[HDCO]/[H <sub>2</sub> CO]	[D <sub>2</sub> CO]/[H <sub>2</sub> CO]
Emission	Fixed at 80 K	5.0	0.81	0.27	16%	5.4%
	Fixed at 45 K	3.8	0.52	0.19	14%	5.0%
	Left as free parameter	3.8	0.48	0.19	13%	5.0%
Absorption	~ 20 K	4	–	0.5	–	12%

since its velocity is almost exactly that of IRAS 16293–2422, it is certainly associated to the source itself. The presence of the component in absorption therefore suggests that the D<sub>2</sub>CO emission is quite extended, and that the relative abundance of D<sub>2</sub>CO increases with the distance from the protostar. This is confirmed by a D<sub>2</sub>CO map of IRAS 162933–2422 (Ceccarelli et al., in prep.).

#### 4. Discussion

Though slightly lower than initially claimed by Ceccarelli et al. (1998), the relative abundance of the D<sub>2</sub>CO in emission towards IRAS 16293–2422 is extremely high (~ 5% with respect to H<sub>2</sub>CO). Such a high formaldehyde deuteration is also seen in the colder gas which absorbs the line at the systemic velocity. The gas temperature *measured* in both the emission and the absorption components (~ 45 K, and 20 K, respectively) is too high to have appreciable deuteration in the gas phase. Standard gas-phase chemical models predict an abundance of HDCO ten times lower, the discrepancy between theory and observations is even much higher for D<sub>2</sub>CO (e.g. Millar et al. 1989). That the observed formaldehyde deuteration is not produced in the gas phase is also supported by the [DCO<sup>+</sup>]/[HCO<sup>+</sup>] ratio observed towards IRAS 16293 (~ 1% – VBJG95). Since the [DCO<sup>+</sup>]/[HCO<sup>+</sup>] ratio reflects the [D]/[H] ratio in the gas phase (e.g. Caselli et al. 1998) the gas-phase deuteration in this source is more than ten times lower than that observed for the formaldehyde.

A natural explanation to the high deuteration of H<sub>2</sub>CO is that D<sub>2</sub>CO (and HDCO) are evaporated from the grain mantles, as already argued in previous works (Turner 1990; Ceccarelli et al. 1998). Models of grain surface chemistry indeed predict high deuteration and high double deuteration of formaldehyde (Tielens 1983; Charnley et al. 1997), provided the source has gone through a cold, dense phase. In the case of a protostar, that phase is readily provided by the pre-collapse period. Hence, the observed high abundances of HDCO and D<sub>2</sub>CO suggest a scenario in which accreted atoms and molecules reacted on grain surfaces during the pre-collapse phase to form hydrogenated (and oxidized) species such as H<sub>2</sub>CO and their deuterated counterparts. Those species being currently released into the gas phase under the influence of the newly formed star.

The abundance ratio found here for D<sub>2</sub>CO is more than an order of magnitude higher than that found in the high-mass star-forming region Orion KL (Turner 1990). If the observed D<sub>2</sub>CO relative abundances indeed reflect the gas phase [D]/[H]

ratio during the pre-collapse, the differing relative abundances between Orion and IRAS 16293–2422 should result from differing physical conditions (density and temperature) during the pre-collapse period. Most probably the temperature is the key parameter: it is quite conceivable that the temperature of the Orion cloud, which harbors many massive protostars, was much higher during the pre-collapse phase of the KL object than in the dark and isolated cloud where IRAS 16293–2422 lies. When the chemistry leading to the formation of high abundances of deuterated species will be better understood, the measure of deuteration levels in protostars may provide a valuable probe of the physical conditions just before the dynamical collapse.

#### 5. Conclusions

This article presents and analyses new multi-transition observations of D<sub>2</sub>CO, HDCO, H<sub>2</sub>CO, and H<sub>2</sub><sup>13</sup>CO towards the low-mass protostar IRAS 16293–2422. The abundance ratio between D<sub>2</sub>CO and H<sub>2</sub>CO is found to be of the order of 5%, while that between HDCO and H<sub>2</sub>CO is about 13–14%. Given the gas temperature (20–50 K), deuteration in the gas phase is unlikely to explain the observed levels of deuteration. Also, the deuteration of the molecular ion HCO<sup>+</sup> (arguably a measure of the [D]/[H] ratio in the gas phase) is found to be an order of magnitude lower than that of the singly deuterated formaldehyde. Hence, the observed D<sub>2</sub>CO is most likely evaporated from the dust grains where it has been accumulated during the dense pre-collapse phase.

In addition to the emission feature, a component in absorption is found that seems to have an even higher D<sub>2</sub>CO relative abundance. This suggests that the D<sub>2</sub>CO is extended around the protostar, and that the D<sub>2</sub>CO abundance ratio increases with the distance to the central source. Recent large scale observations do confirm this hypothesis (Ceccarelli et al., in prep.).

*Acknowledgements.* We thank the IRAM and JCMT staffs in Spain and Hawaii for their assistance with the observations, and the IRAM and JCMT Program Committees for their award of observing time. Stimulating discussions with Emmanuel Dartois are gratefully acknowledged.

#### References

- Brown P.D., Millar T.J., 1989, MNRAS 240, 25
- Caselli P., Walmsley C.M., Terzieva R., Herbst E., 1998, ApJ 499, 234
- Ceccarelli C., Castets A., Loinard L., Caux E., Tielens A.G.G.M., 1998, A&A 338, L43.

- Ceccarelli C., Loinard L., Castets A., Tielens A.G.G.M., Caux E., 2000, *A&A* 357, L9
- Charnley S.B., Tielens A.G.G.M., Rodgers S.D., 1997, *ApJ* 482, L203
- van Dishoeck E.F., Blake G.A., Jansen D.J., Groesbeck T.D., 1995, *ApJ* 447, 760
- Goldsmith P.F., Langer W.D. 1999, *ApJ* 517, 209
- Keene J., Schilke P., Kooi J., Lis D.C., Mehringer D.M., Phillips T.G., 1998, *ApJ* 494, L107
- Langer W.D., Graedel T.E., Frerking M.A., Armentrout P.B., 1984, *ApJ* 277, L581
- Millar T.J., Bennett A., Herbst E. 1989, *ApJ* 340, 906.
- Roueff E., Tiné S., Coudert L.H., et al., 2000, *A&A* 354, L63.
- Tielens A.G.G.M., 1983, *A&A* 119, 177
- Turner B.E., 1990, *ApJ* 362, L29
- Willacy K., Millar T.J., 1998, *MNRAS* 298, 562